Stanford Exploration Project, Report 75, November 17, 1997, pages 121–135

Stanford Exploration Project, Report 75, November 17, 1997, pages 121–135

Least squares imaging, datuming, and interpolation using the wave equation

Jun Ji[1]

keywords: *modeling, least squares, imaging*

ABSTRACT

Though the continuous wave equation defines a unitary operator, many operators based on it are not unitary because many approximations are made to be implemented numerically in finite and discrete space. The nonunitary property of the operators produces many artifacts in the solution space when is applied to data that was generated by a continuous unitary operator, such as real seismic data. This paper presents a method of reducing these kinds of artifacts in migration, datuming, and interpolation by using the technique of a least-squares optimization.

INTRODUCTION

One approach to producing a good subsurface image by a migration technique is to find an operator that resembles the continuous wave equation as close as possible. Even if the operator very closely resembles to the wave equation, the data obtained in a survey is discrete in form and is limited both in the apertures and in the sampling intervals. In order to overcome these problems, the extending common-midpoint gather (Claerbout, 1990) and trace interpolation techniques (Claerbout, 1992a: Ji, 1992) have been applied.

Another approach to obtaining a good image without artifacts might be an optimization technique that finds the image that best fits the data for a given modeling operator. If the problem is datuming, the operator can be an extrapolation operator from one surface to another. This paper presents an approach to obtaining the optimized images and datumed wavefield for several extrapolation operators in the least-squares sense. It then introduces the application of an interpolation technique.

[1]**email:** not available

LEAST-SQUARES IMAGING

The exploding reflector model provides the linear relation between the subsurface image and the wavefield on the surface. In forward modeling, the input is the subsurface image and the output is the wavefield on the surface. The migration is the conjugate operation to the forward modeling (Claerbout, 1992a). If the modeling operator is a unitary operator, the migration operator, which is the conjugate of the modeling operator, will backproject the wavefield to the subsurface image, which results in the original input of the modeling. However, in reality the forward operator is the continuous wave equation for a given earth model, and the backprojection operator, which is migration operator, is not the conjugate to the forward operator. Instead we use an operator that is conjugate to an approximated forward operator like the Kirchhoff, phase shift, and finite-difference method. This discrepancy along with the finite and the discrete limits produces many artifacts on the image after migration.

The forward modeling can be simply formulated as

$$\mathbf{d} = \mathbf{SWm} \tag{1}$$

where $\mathbf{W}$ is the wave equation operator that does the forward modeling, $\mathbf{m}$ is the continuous model space, $\mathbf{S}$ is the truncating and sampling operator that simulates the finite and discrete seismic survey, and $\mathbf{d}$ is the data we obtain in reality. In conventional migration, we approximate the forward operator $\mathbf{SW}$ as

$$\mathbf{S\tilde{W}} \simeq \mathbf{SW} \tag{2}$$

where $\tilde{\mathbf{W}}$ represents an approximated forward modeling operator. Therefore, the conventional migration actually solve the problem as follows

$$\hat{\mathbf{m}} \simeq \tilde{\mathbf{W}}'\mathbf{S}'\mathbf{d} = \tilde{\mathbf{W}}'\mathbf{S}'\mathbf{SWm} \tag{3}$$

Even though the sampling interval is small and the aperture is large, which makes the operator $\mathbf{S}$ identity matrix, some artifacts might be appeared if the operator $\tilde{\mathbf{W}}$ differs from W. Thus, both the accurate approximation for the wave equation and the wide aperture and the dense sampling are important to get a good image.

The other approach to getting a good image for a given sampling interval and a given poor but cheap operator might be to use the least-squares optimization technique to find the best image. To solve formally for the unknown $\mathbf{m}$ in the least-squares sense, we solve the normal equation as follows:

$$\hat{\mathbf{m}} = (\tilde{\mathbf{W}}'\mathbf{S}'\mathbf{S}\tilde{\mathbf{W}})^{-1}\tilde{\mathbf{W}}'\mathbf{S}'\mathbf{d} \tag{4}$$

This may not recover the original image $\mathbf{m}$ because $\mathbf{d}$ was generated by the operator $\mathbf{SW}$ which differs from the operator $\mathbf{S\tilde{W}}$. If we assume that we have approximated the wave equation very accurately, that is $\tilde{\mathbf{W}} = \mathbf{W}$, and the only problem that causes artifacts is due to the operator $\mathbf{S}$, we are solving correct normal equation as

$$\hat{\mathbf{m}} = (\mathbf{W}'\mathbf{S}'\mathbf{SW})^{-1}\mathbf{W}'\mathbf{S}'\mathbf{d}. \tag{5}$$

Usually the operator $\mathbf{S\tilde{W}}$ is too large in size to solve the inversion of $(\mathbf{\tilde{W}'S'S\tilde{W}})$. An alternative might be an iterative inversion, with the hope of a fast convergence, such as the conjugate gradient method. Fortunately, the initial guess for the conjugate gradient is conventional migration, which is the image after applying the conjugate operator of the forward operator. It gets very close to the solution except for some artifacts. We can expect a fast convergence and a close solution obtained in a few iterations. The object function we want to minimize using the conjugate gradient can be formulated as follows :

$$\min_{\mathbf{m}} ||\hat{\mathbf{d}} - \mathbf{S\tilde{W}m}|| \tag{6}$$

where $\hat{\mathbf{d}}$ represents the data generated by the forward operator $\mathbf{S\tilde{W}}$ and this operator could be any modeling operator like the Kirchhoff, phase-shift, or finite-difference method.

Kirchhoff migration in constant velocity

For Kirchhoff migration, I used Claerbout's **kirchfast()** subroutine (Claerbout, 1992b). The **kirchfast()** subroutine is the simplest zero-offset Kirchhoff migration program I could find, but it produces many artifacts when is applied to a sparsely sampled data because of the nearest neighbor interpolation. Figure 1(a) shows a simple model with a syncline image. The Kirchhoff modeling for the model [Figure 1(a)] is shown in Figure 1(b), and the migration result is shown in Figure 1(c). The image in Figure 1(c) is very blurred compared to the original image. We can suppress this artifact by the least-squares imaging; the result is shown in Figure 1(d). The image in Figure 1(d) is very close to the original image, without any artifacts. This result was obtained after only 5 iterations of the conjugate gradient algorithm.

For more realistic synthetic model, I used Claerbout's synthetic model, which has a very complicated geological model, as shown in Figure 2(a). Figure 2(b) shows the synthetic data generated by the subroutine **kirchfast()**, and Figure 2(c) the result of migration. The image after migration is smoother than the original image. This suggests applying an $|\omega|$ filter to recover the high frequency. The image after the least-squares inversion, shown in Figure 2(d), contains more high frequency than the image after migration. The frequency recovery in the image after migration and inversion is shown in Figure 3. We can see that the spectrum of the image obtained by the least-squares imaging is very close to the spectrum of the original image. Figure 4 illustrates the same experiment as Figure 2, except that the sampling interval is two times that of the sampling interval of the model used in Figure 2. The image after migration in Figure 2(c) shows artifacts because of the change in the sampling interval. But the image obtained by the least-squares imaging, Figure 2(d), is still clear.

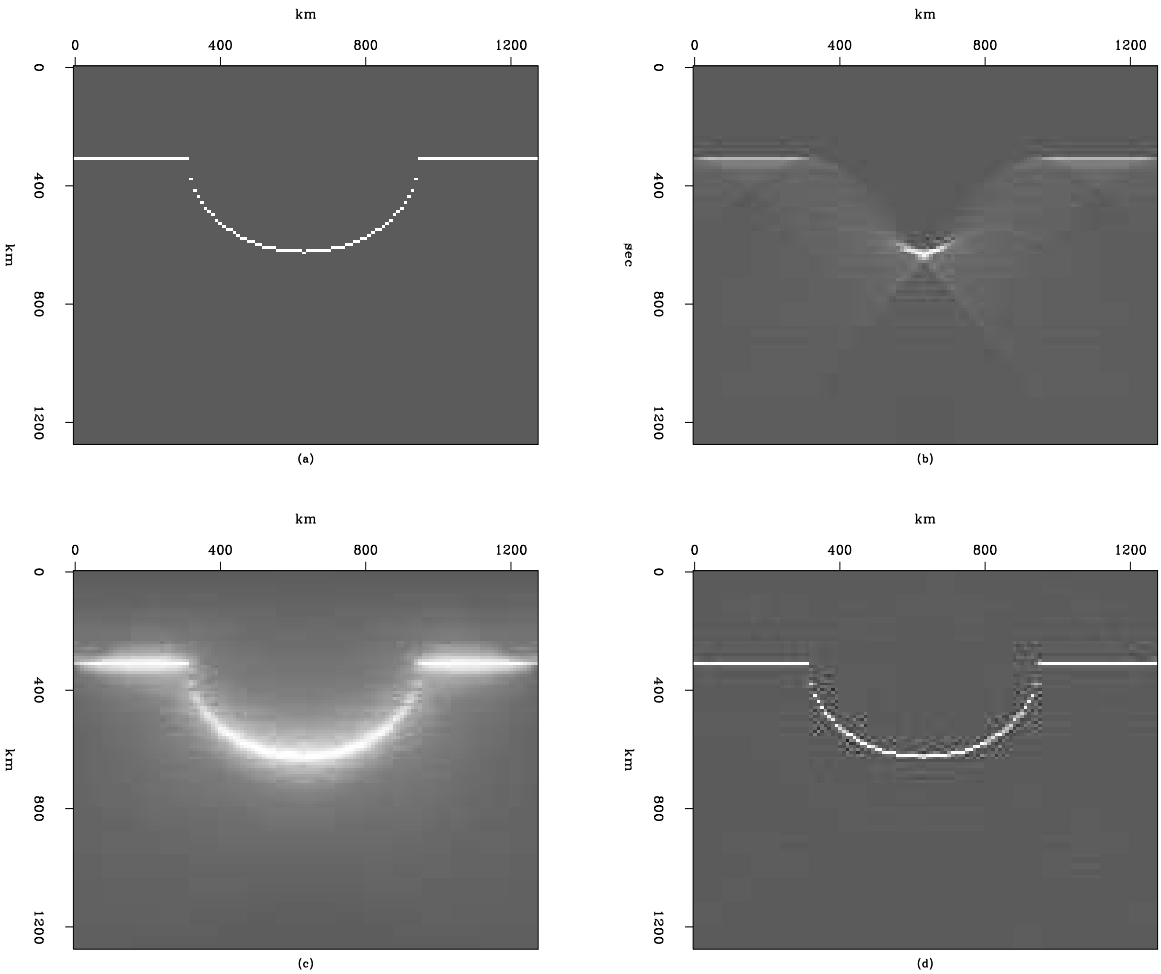

Figure 1: Least-squares Kirchhoff imaging: **(a)** Synthetic image model containing a syncline reflector, **(b)** Kirchhoff modeling, **(c)** Kirchhoff migration for (b), **(d)** Least-squares Kirchhoff imaging for (b) (after 5 iterations of the conjugate gradient algorithm). jun2-Kirmiginv [NR]

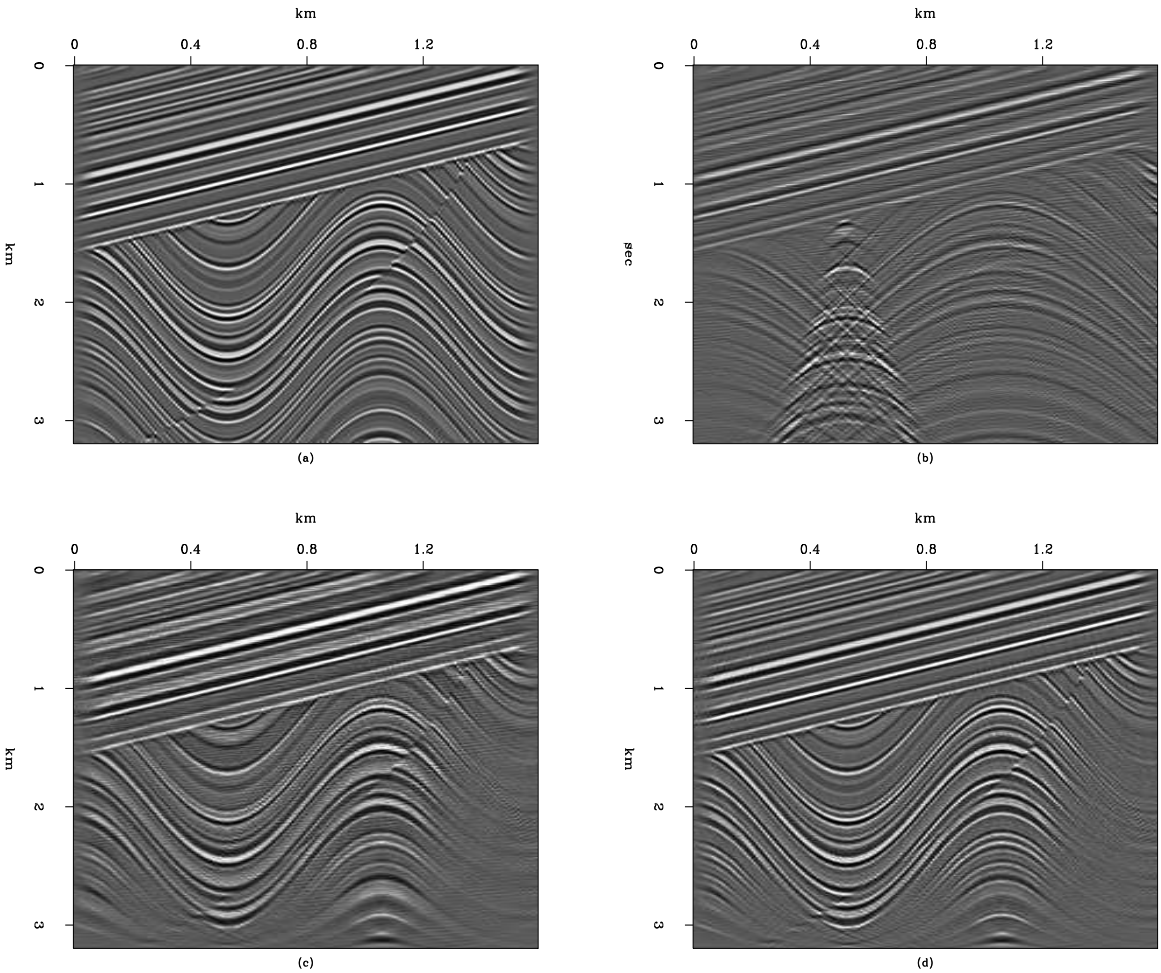

Figure 2: Kirchhoff inversion: **(a)** Synthetic image model with a syncline (nz=128 and nx=200), **(b)** Kirchhoff modeling, **(c)** Kirchhoff migration for (b), **(d)** Least-squares Kirchhoff inversion for (b) (after 10 iterations of the conjugate gradient algorithm). jun2-kirinv3 [NR]

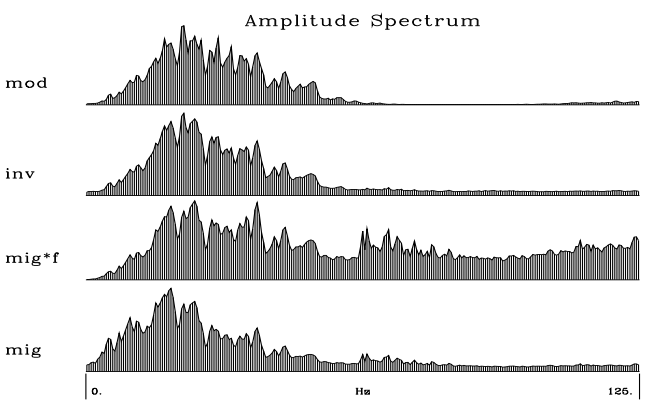

Figure 3: Spectrum recovery after migration and inversion. From the top: The spectrum of the original image, of the inversed image, of the migration image times frequency, and of the migration image. jun2-kirspec3 [NR]

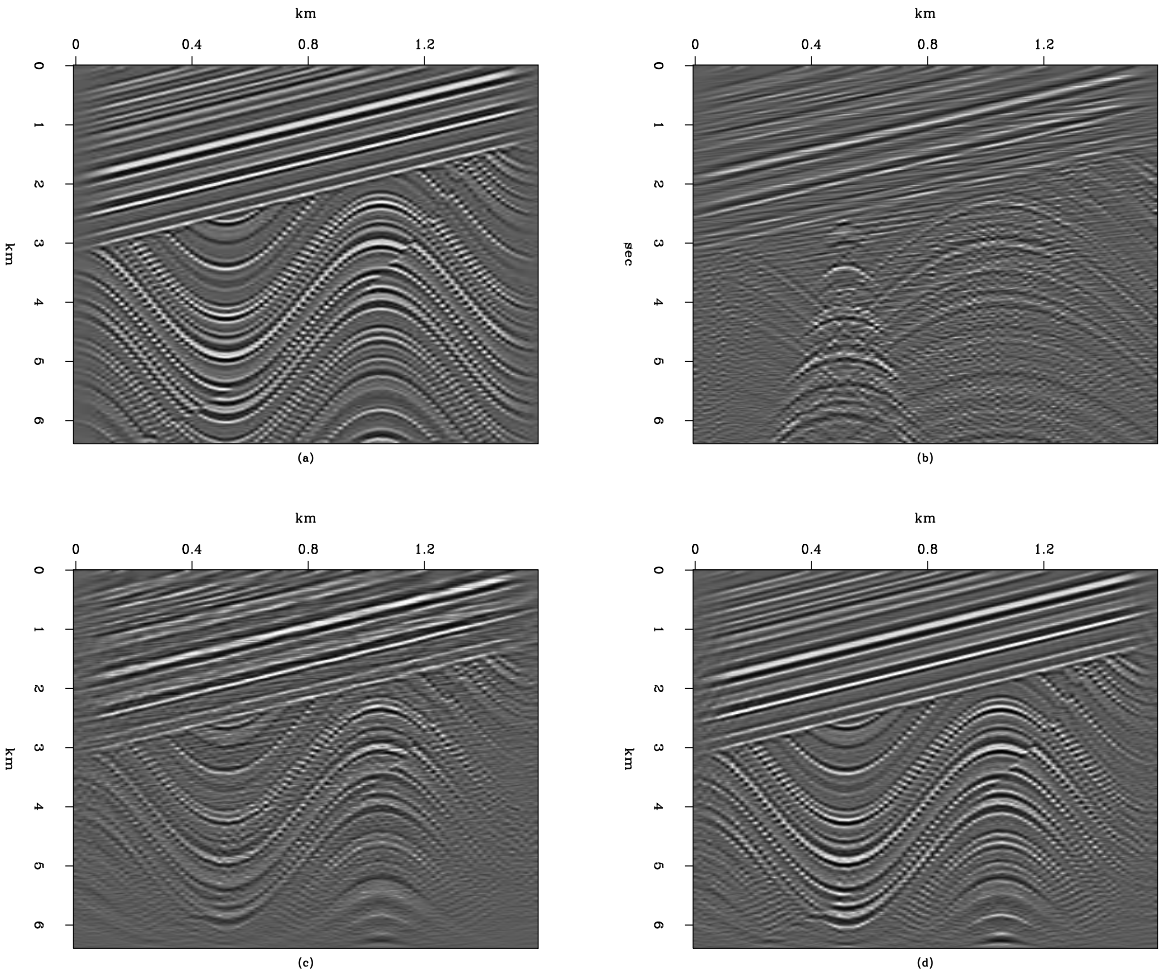

Figure 4: Kirchhoff inversion: **(a)** Synthetic image model with a syncline (nz=128 and nx=100), **(b)** Kirchhoff modeling, **(c)** Kirchhoff migration for (b), **(d)** Least-squares Kirchhoff inversion for (b) (after 10 iterations of the conjugate gradient algorithm). jun2-kirinv2 [NR]

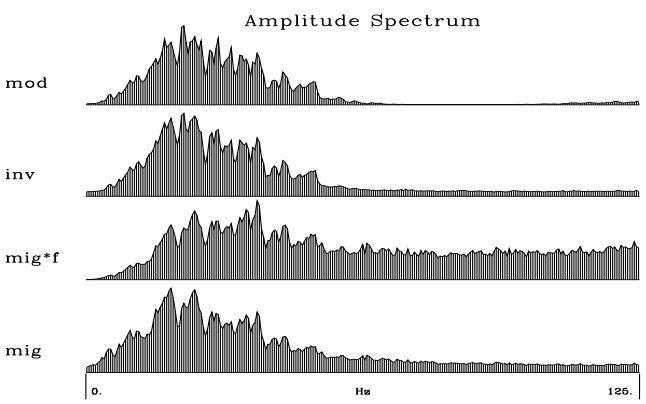

Figure 5: Spectrum recovery after migration and inversion. From the top: The spectrum of the original image, of the inversed image, of the migration image times frequency, and of the migration image. jun2-kirspec2 [NR]

Gazdag migration in v(z)

Gazdag modeling and migration is not a unitary operator for depth-variable velocity. As a result, we lose steep dip components of the image after migration. The least-squares imaging method can be used instead to recover the high dip components. Now the operator in equation (2) becomes the Gazdag modeling operator. Figure 6(a) shows the velocity function used in the experiment, and the image in the model has the same syncline reflector as Figure 1(a). The result of the forward Gazdag modeling is shown in Figure 6(b). The image obtained by the migration of this data is shown in Figure 6(c) and we can see that the steep dip components is weakly imaged in comparison to the original model. The image obtained by the least-squares imaging of the same data, shown in Figure 6(d), shows more steep dip energy.

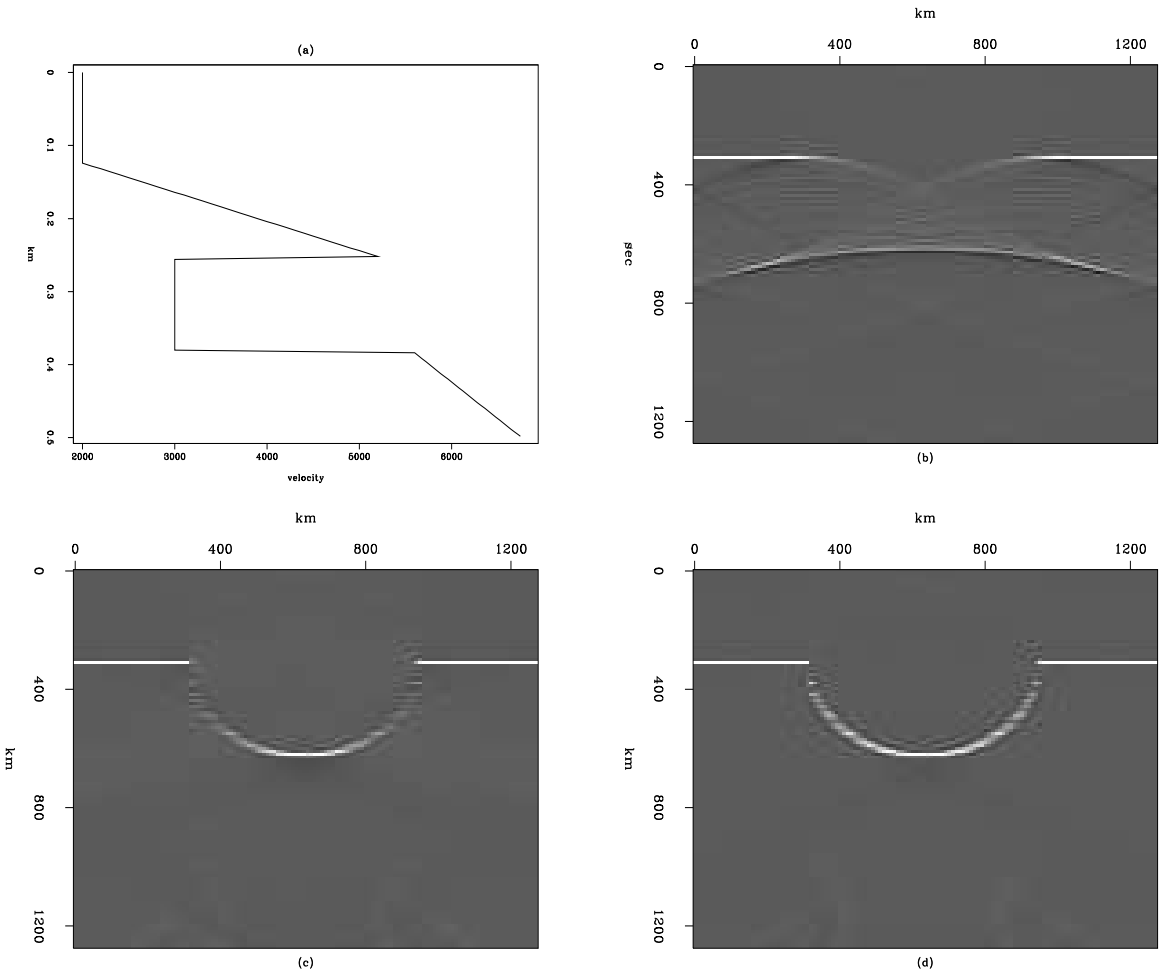

Figure 6: Least-squares Gazdag imaging: **(a)** The velocity model for the syncline reflector shown in Figure 1(a), **(b)** Gazdag modeling, **(c)** The image obtained by the Gazdag migration for (b), **(d)** The image obtained by the least-squares Gazdag imaging for (b) (after 10 iterations). jun2-Gazmiginv [NR]

Gazdag migration from an irregular surface

An algorithm for depth migration when the surface is nonflat is presented by Ji and Claerbout (1992) elsewhere in this report. If the surface fluctuates severely, the aperture of the wavefield varies with the surface. The varying aperture along the surface results in an amplitude change in the image. Figure 7(c) shows this effect caused by the undulating topography shown in Figure 7(a). In the portion of flat surface the reflector has imaged correctly, but in the portion of nonflat surface the image shows slight amplitude change with some background noise. The result of the least-squares imaging is shown in Figure 7(d); it is more correct than the image after migration.

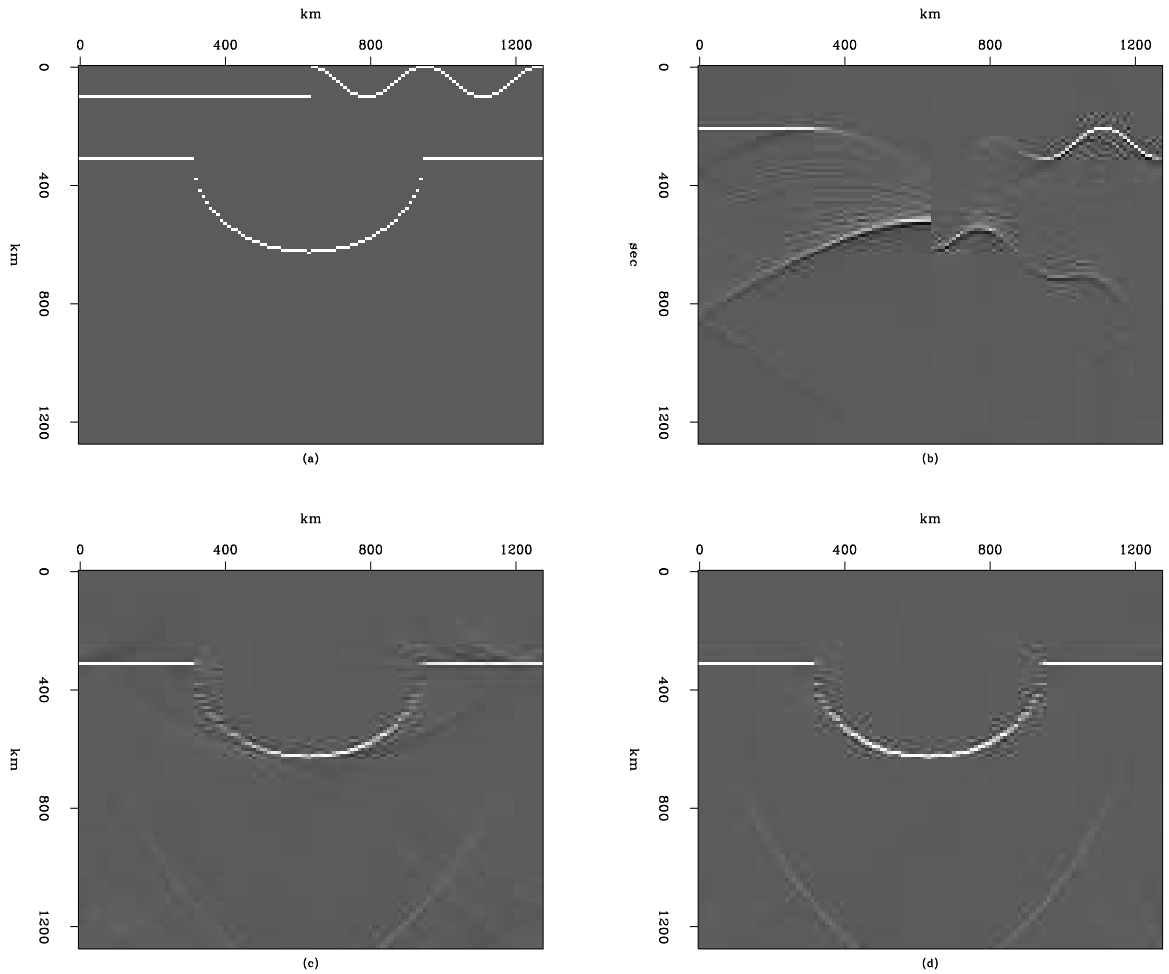

Figure 7: Least-squares Gazdag imaging from an irregular surface: **(a)** A syncline reflector model under the undulating surface (upper white line), **(b)** The data obtained by the Gazdag modeling using the algorithm introduced by Ji and Claerbout (1992), **(c)** The image obtained by the Gazdag migration for (b), **(d)** The image obtained by the least-squares Gazdag imaging for (b) (after 10 iterations). jun2-Topomiginv [NR]

Finite-difference migration in v(x,z)

For the finite-difference migration, I tested the 45-degree equation in (ω, x, z). The velocity model used has a constant gradient from the left upper side to the right lower side, which is shown in Figure 8(a). Using this velocity model, a syncline reflector was modeled by the finite-difference method using the 45-degree equation and is shown in Figure 8(b). The migration result obtained by the conjugate of the forward modeling is shown in Figure 8(c). The reflector has clearly imaged except for background artifacts which seem to be caused by the boundary reflection. Figure 8(d) shows that we can suppress these artifacts by using the least-squares imaging method.

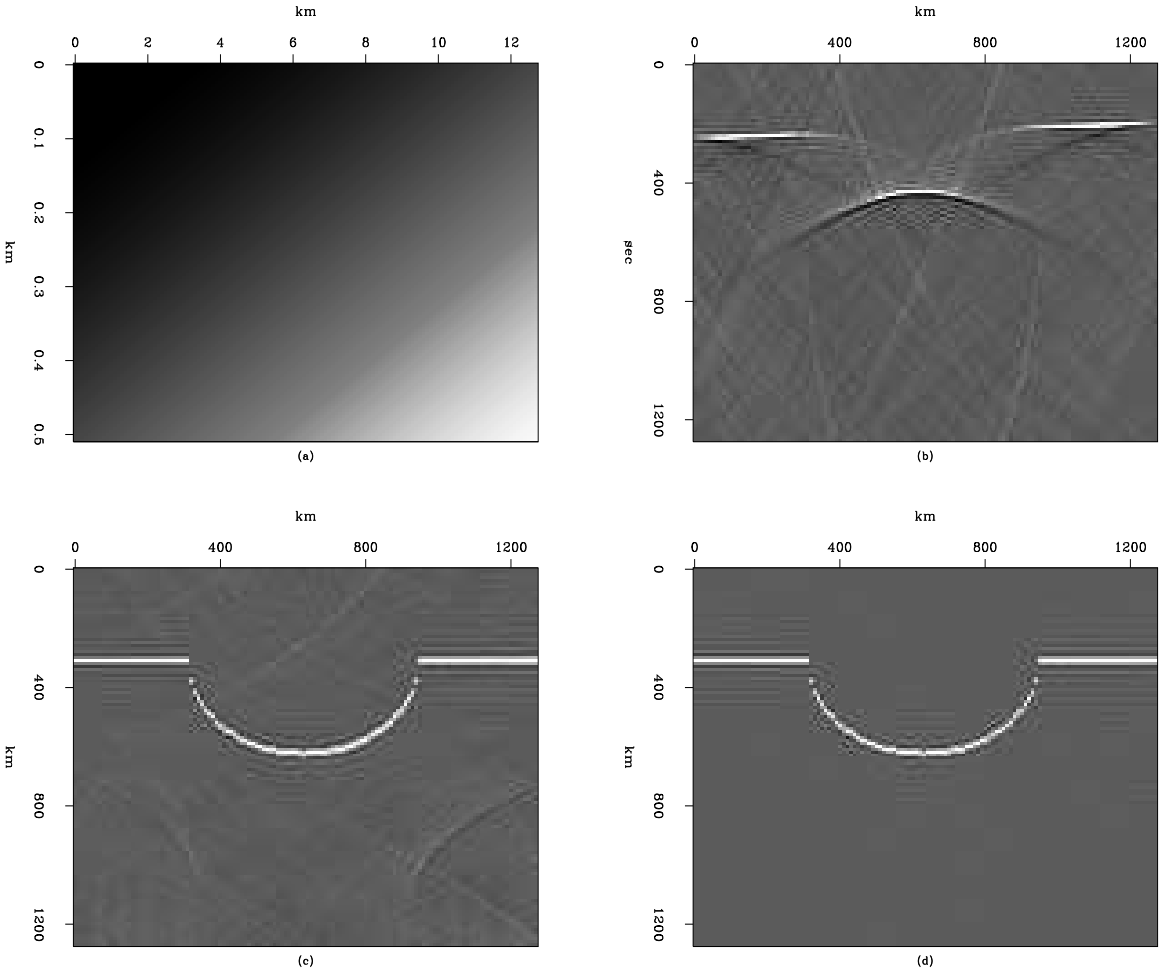

Figure 8: Least-squares finite-difference imaging in (ω, x, z): **(a)** The velocity model with a syncline reflector shown in Figure 1(a), **(b)** 45-degree finite-difference modeling, **(c)** The image obtained by the 45-degree finite-difference migration for (b), **(d)** The image obtained by the least-squares finite-difference imaging for (b) (after 10 iterations). jun2-Wxz45miginv [NR]

LEAST-SQUARES DATUMING

Datuming is a method of processing to extrapolate a known wavefield at a specified datum of arbitrary shape to another specified datum, also of arbitrary shape. Ji and Claerbout (1992) presented a datuming algorithm based on the phase-shift depth extrapolation elsewhere in this report. In the datuming problem, we use upward and downward extrapolation operators instead of the modeling and migration operators. For a given wavefield on the irregular surface, we can estimate new wavefield on a datum by minimizing the errors between the given input and the data modeled by the extrapolation, as follows:

$$\min_{\mathbf{d_0}} ||\mathbf{d} - \mathbf{E}\mathbf{d_0}|| \tag{7}$$

where $\mathbf{d}$ is a given wavefield on an irregular topography, $\mathbf{d_0}$ is a wavefield on a new datum, and $\mathbf{E}$ represents an extrapolation operator either upward or downward. For example, if a new datum is located above the given datum, the extrapolation operator $\mathbf{E}$ will be the downward extrapolation operator.

For demonstration, the phase shift datuming operator, explained by Ji and Claerbout (1992), was used. Figure 9(a) is the wavefield on a datum. This wavefield was extrapolated to the nonflat surface shown in Figure 7(a), and the wavefield on the nonflat surface is shown in Figure 9(b). The purpose is to datum the wavefield to the original surface. By using the downward extrapolation operator, I obtained datumed wavefield; the result is shown in Figure 9(c). Compared to the original wavefield, the datumed wavefield is correctly positioned, but you can see that the amplitude of the datumed wavefield is different from that of the original wavefield. Figure 9(d) shows the datumed wavefield obtained by using the least-squares datuming method. It has a very nice amplitude recovery.

LEAST-SQUARES INTERPOLATION

The forward modeling for sparsely sampled data can be formulated by applying a subsampling operator to the exploding reflector modeling operator as follows:

$$\mathbf{d} = \mathbf{S_2}\mathbf{S}\tilde{\mathbf{W}}\mathbf{m} \tag{8}$$

where data $\mathbf{d}$ and image $\mathbf{m}$ have different lengths in the space direction because of the subsampling operator $\mathbf{S_2}$, and the exploding reflector modeling operator $\mathbf{S}\tilde{\mathbf{W}}$, the same operator as equation (2), can be any modeling operator such as Kirchhoff, phase-shift, or finite-difference. For a given sparsely sampled wavefield, we can estimate a dense image by minimizing the error between the given wavefield and the wavefield modeled by the modeling equation(7), which is as follows:

$$\min_{\mathbf{m}} ||\mathbf{d} - \mathbf{S_2}\mathbf{S}\tilde{\mathbf{W}}\mathbf{m}|| \tag{9}$$

Experiments were done using the Kirchhoff and phase-shift operators. For a simple syncline reflector shown in Figure 1(a), a synthetic model was generated using the

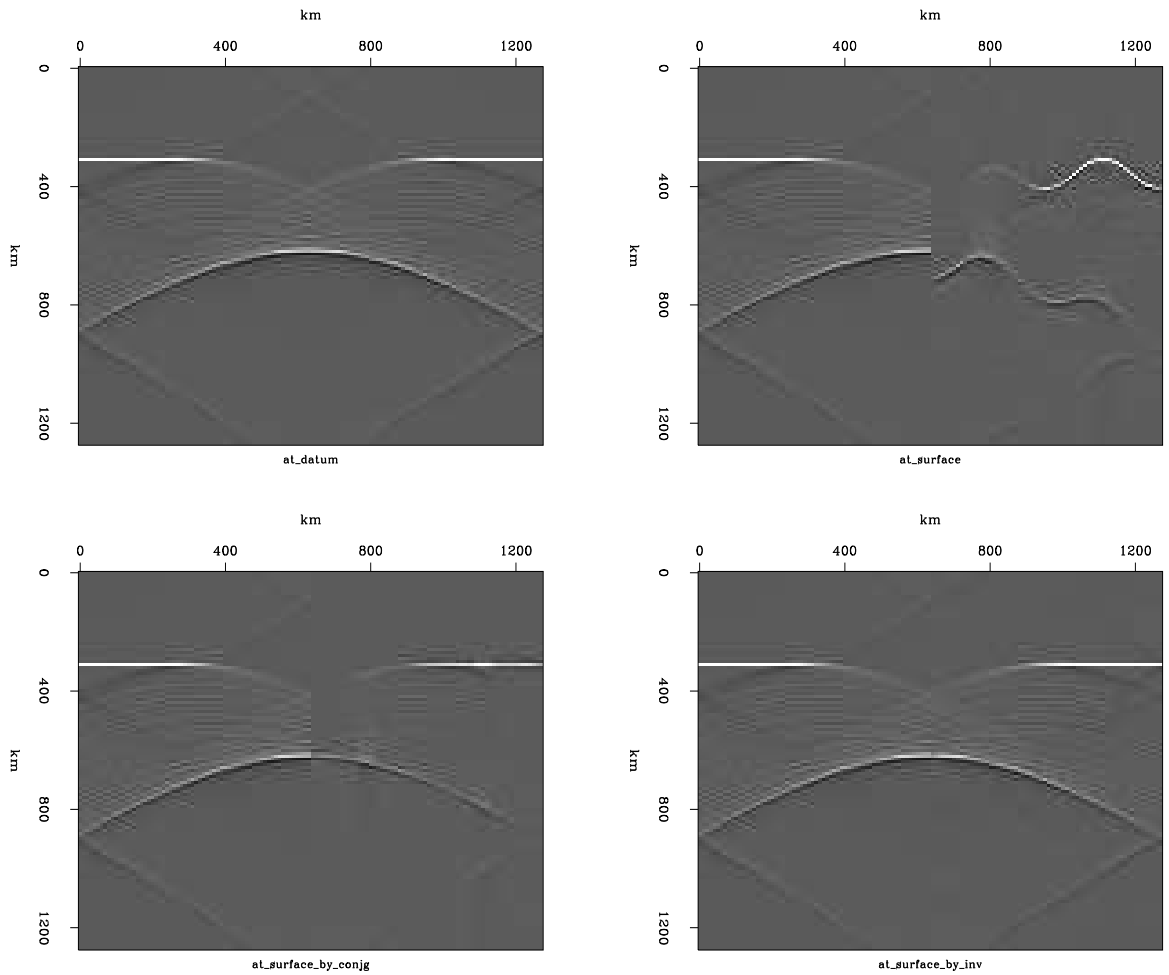

Figure 9: Least-squares inverse datuming: **(a)** Wave field on the datum surface. **(b)** Wave field on the undulating surface shown in Figure 7(a), **(c)** Datumed wavefield from the undulating surface shown in (b), **(d)** wavefield obtained by the least-squares inverse datuming from the undulating surface shown in (b) (after 10 iterations). jun2-Dtminv [NR]

Kirchhoff modeling operator and the subsampled by zapping every other trace. The result of modeling is shown in Figure 10(b). By applying the conjugate operator, $\mathbf{W}'\mathbf{S}'$, to the subsampled data, we get an interpolated image, as shown in Figure 10(c). It is very difficult to distinguish the effect of the subsampling operator from the artifacts of the Kirchhoff operator, but we can see that this image is very similar to the image obtained without the subsampling operator shown in Figure 1(c). The image obtained by the least-squares interpolation is shown in Figure 10(d); it closely resembles the image obtained from the data without subsampling.

Another experiment done using the Gazdag operator is shown in Figure 11. This result also closely resembles that for the images without subsampling. The reason may be that the wavefront healing effect during the extrapolation.

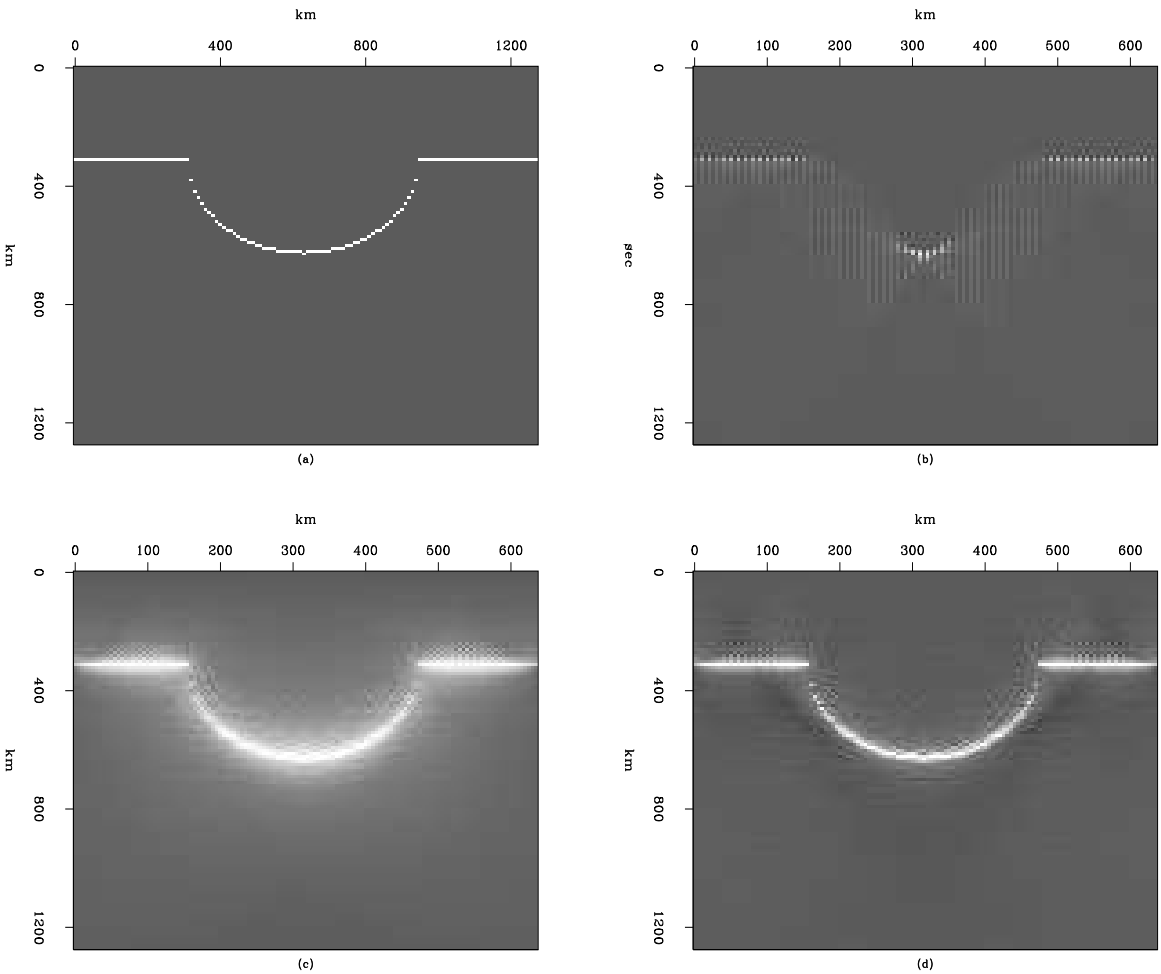

Figure 10: Least-squares Kirchhoff interpolation: **(a)** The original image used to generate the subsampled wavefield shown in Figure 1(b), **(b)** The subsampled wavefield. **(c)** The interpolated subsurface image obtained by Kirchhoff migration with a subsampling operator, **(d)** The interpolated subsurface image obtained by least-squares Kirchhoff interpolation (after 10 iterations). jun2-Kirint [NR]

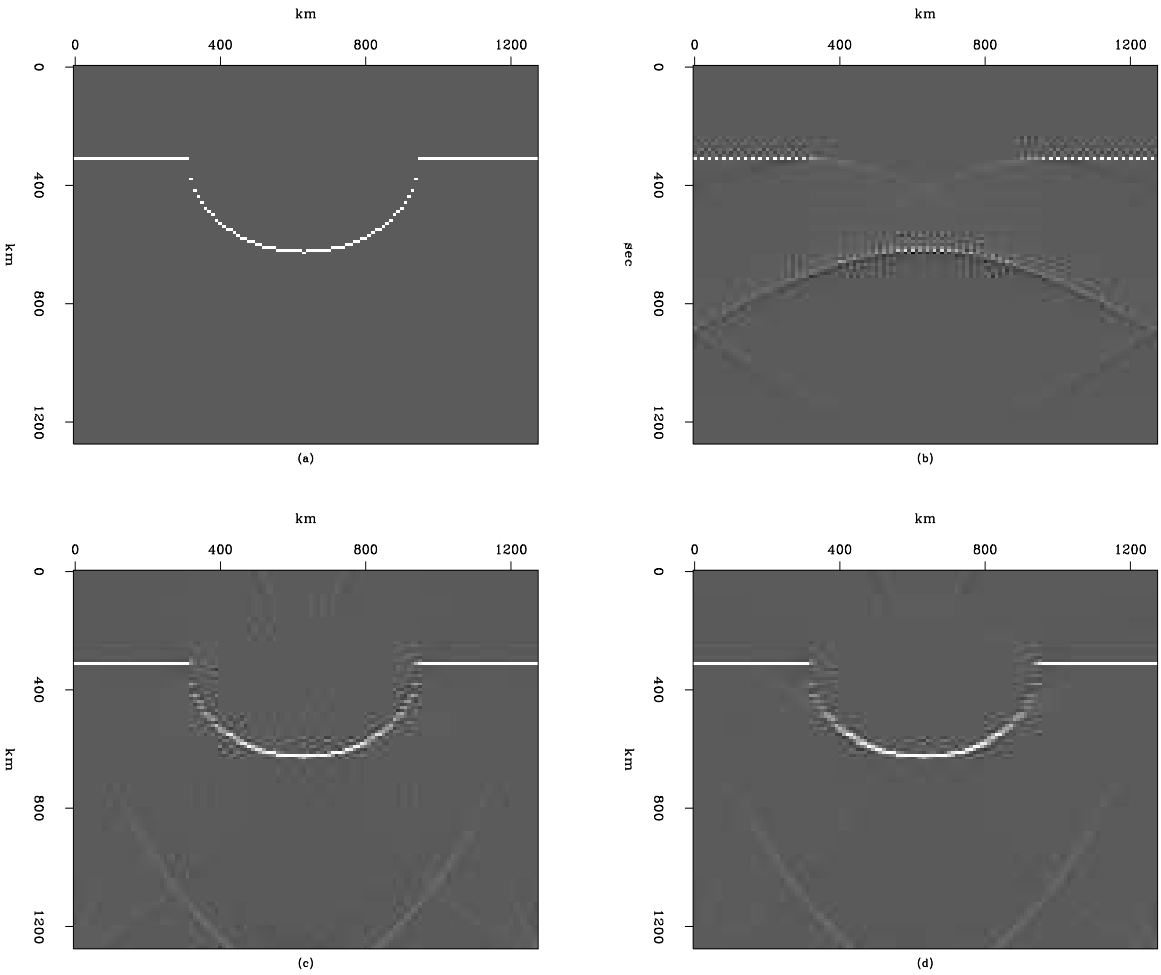

Figure 11: Least-squares interpolation with Gazdag operator: **(a)** The original wavefield generated by Gazdag modeling for the synthetic model shown in Figure 1(a), **(b)** The subsampled wavefield obtained by zapping every other trace in Figure 11(a), **(c)** The interpolated subsurface image obtained by Gazdag migration, **(d)** The interpolated subsurface image obtained by least-squares Gazdag migration (after 10 iterations). jun2-Gazint [NR]

CONCLUSION

Though the wave equation is a unitary operator, many operators based on it are not unitary because many approximations are made to be implemented numerically in finite and discrete space. The nonunitary property of the operators produce many artifacts in the solution space when the property is applied to data that were produced by a continuous unitary operator, such as real seismic data. This paper presents a method of reducing these artifacts in migration, datuming, and interpolation by using the technique of least-squares optimization.

ACKNOWLEDGMENTS

I would like to thank Jon Claerbout for sharing his codes.

REFERENCES

Claerbout, J. F., 1990, Extending a CMP gather by optimization in velocity space: SEP–**67**, 43–49.

Claerbout, J. F., 1992a, Earth Soundings Analysis: Processing versus Inversion: Blackwell Scientific.

Claerbout, J. F., 1992b, Introduction to Kirchhoff migration programs: SEP–**73**, 361–366.

Ji, J., 1992, Trace interpolation by simulating a prediction-error filter: SEP–**73**, 203–220.

Ji, J., and Claerbout, J. F., 1992, Phase shift datuming and migration from an irregular surface: SEP–**75**, 169–182.